Peer-reviewed version available at Entropy 2018, 20, 929; doi:10.3390/e20120929

Article

Entropy Density Acceleration and Minimum Dissipation Principle: Correlation with Heat and Matter Transfer in Glucose Catabolism

Roberto Zivieri[1,*], **Nicola Pacini**[2,3]

[1]Department of Mathematical and Computer Sciences, Physical Sciences and Earth Sciences, University of Messina, Messina, Italy

[2] Laboratory of Biochemistry F. Pacini, Reggio Calabria, Italy;

[3]Department of General Surgery and Senology, University Hospital Company, Catania, Italy;
pacini.biochemistry@gmail.com

* Correspondence: roberto.zivieri@unife.it; Tel.: +39-0532-974213

Academic Editor: Prof. Dr. José Miguel Mateos Roco

Abstract: The heat and matter transfer during glucose catabolism in living systems and their relation with entropy production are a challenging subject of the classical thermodynamics applied to biology. In this respect, an analogy between mechanics and thermodynamics has been performed via the definition of the entropy density acceleration expressed by the time derivative of the rate of entropy density and related to heat and matter transfer in minimum living systems. Cells are regarded as open thermodynamic systems that exchange heat and matter resulting from irreversible processes with the intercellular environment. Prigogine's minimum energy dissipation principle is reformulated using the notion of entropy density acceleration applied to glucose catabolism. It is shown that, for out-of-equilibrium states, the calculated entropy density acceleration is finite and negative and approaches as a function of time a zero value at global thermodynamic equilibrium for heat and matter transfer independently of the cell type and the metabolic pathway. These results could be important for a deeper understanding of entropy generation and its correlation with heat transfer in cell biology with special regard to glucose catabolism representing the prototype of irreversible reactions and a crucial metabolic pathway in stem cells and cancer stem cells.

Keywords: Entropy generation; entropy acceleration; glucose catabolism; irreversible reactions; heat transfer; matter transfer; cancer biology; stem cell biology

1. Introduction

In nature, irreversible processes play a crucial role in maintenance of life for their special chemical and physical features [1-4]. Regarding this, it is well-known that products of irreversible reactions are characterized by a chemical stability that gives them a temporal stabilization and a precise time arrow. Hence, it is very interesting to understand the thermodynamics of irreversible reactions

occurring in minimum living systems investigating the relation between irreversibility and information. The physical quantity able to describe in a unitary way the irreversibility and information in minimum living systems is entropy [5]. In this respect, very recently, it has been proposed a new variable, the entropy of entropy, enabling to measure the complexity for biological systems through the combination of the multiscale entropy analysis and an alternate measure of information, called the superinformation [6]. Within Prigogine's framework of non-equilibrium thermodynamics, the local entropy production as a function of time is a key quantity strictly related to the energy dissipation of a system that continuously decreases during development, growing and aging [7,8].

Among irreversible reactions in minimum living systems the most representative are the ones occurring in glucose catabolism characterized by both lactic acid fermentation and respiration metabolic pathways. Since the observation of a prevalent lactic acid fermentation in cancer cells, the so-called Warburg effect or aerobic glycolysis, many efforts were done to understand the origin of this behaviour in cancer cells and cancer stem cells [9-11]. On the other hand, in the last years also the study of the metabolic network and of the mitochondria network have received a special attention [12].

In recent years, it has also been highlighted and demonstrated the strict connection between thermodynamic irreversibility and information resulting from the strong influence of metabolic patterns on genetic and epigenetic patterns in biological systems, the study of the generation of entropy in normal, cancer and stem cells [11-15]. Attention should focus not only on cell biology but also on the thermodynamic description of cells and of the living systems because this different perspective could offer a unitary view of metabolomics, genomics and epigenomics. In other words, the measurement of entropy flow and the study of the thermodynamic behaviour of living systems could allow the measurement of a finite quantity represented by entropy, which correlates the many different aspects of life networks. Indeed, all subsystems of the complex cellular building are joined together by a unified thermodynamic time arrow and must follow the same behaviour, that is, the global thermodynamic behaviour coincides with the one of all the subsystems of the considered object [16, 17].

Entropy generation due to heat and matter transfer in cells has been investigated in terms of Prigogine's rate of entropy production [18]. For example, entropy production may select non-equilibrium states in multi-stable systems [19], while reaction-diffusion thermodynamics and entropy production may constrain organism performance at higher temperatures yielding optimal temperatures at which biochemical reactions occurr [20]. Generally, entropy generation occurs in non-equilibrium systems that can be described, for instance, by means of stochastic Langevin differential equation and Fokker-Planck equation [21-23].

An important debate on this topic is about the possible compatibility of the maximum and the minimum entropy production principle or if one of the two principles could be selected in relation to the boundary conditions [24]. The proof and validity of the maximum entropy production principle was debated so far [25-33] and, for a part of the community, is still an open question with several attempts to disprove it. However, very recently a convincing argument in its favour in terms of stochastic thermodynamics has solved the apparent contradictions of the maximum entropy production principle and shown that is not in incompatible with the principle of minimum entropy production [19]. The latter is fulfilled when thermodynamic systems that are close to equilibrium flow towards the global thermodynamic equilibrium when the rate of entropy density production reaches its minimum value (zero value). This scheme can be applied to any thermodynamic system including irreversible processes in minimum living systems like cells behaving as open systems and reversibly exchanging both energy, in the form of heat, and matter with the intercellular environment.

In our recent works on the subject [34, 35], we have studied not only the usual local entropy production defined, in our framework, rate of internal entropy density production (RIEDP) but also the rate of external entropy density production (REEDP) that is related to heat and matter flows from the cell to the environment due to irreversible processes occurring inside cells. Both contributions reduce with increasing time and vanish at global thermodynamic equilibrium. REEDP is usually called in the literature entropy flow or entropy flow rate [7, 18, 19,22] to indicate the entropy

generated by flows of heat and matter either from the system to the environment or from the environment to the system. However, in our framework, restricted to the entropy generation of a single cell, the REEDP is referred to the rate of entropy density production in the intercellular environment due to the irreversible processes occurring inside the cell. In this respect, we have not considered the flows of heat and matter from the environment towards the cell that would correspond to a negative rate for the environment (but positive for the cell) and a resulting negative REEDP.

We have already proved that both RIEDP and REEDP fulfil Prigogine's minimum energy dissipation principle [34, 35] that corresponds to the minimum rate of entropy production principle. Let us introduce a dissipative function $\Psi = T\, dS_i/dt$ where S_i is the entropy of the system with T the temperature. We get $d\Psi/dt \leq 0$ that tends to be minimum (zero) in a steady-state (and as a special case of steady state at global thermodynamic equilibrium) [7]. In this study, we prove Prigogine's minimum energy dissipation principle via the calculation of the time derivative of the rate of entropy density production that we define as the entropy density acceleration generated by heat and matter transfer inside cells and with the intercellular environment in irreversible reactions such as the ones characterizing glucose catabolism. In this way, we reformulate Prigogine's minimum energy dissipation principle by means of the calculation of the entropy density acceleration inside and outside a normal or cancer cell performing also the derivative of the REEDP or entropy flow showing that the acceleration both inside and outside the cell approaches zero at global thermodynamic equilibrium. These calculations allow us to understand better the entity of the entropy production at the starting instants of time of the irreversible processes when the system is out-of-equilibrium and to strengthen the principle of minimum entropy production at global thermodynamic equilibrium and its strict relation with the minimum energy dissipation principle.

The key result of this work is the rigorous demonstration, by means of analytical and numerical calculations, of the reduction of entropy density acceleration with increasing time and its vanishing at global thermodynamic equilibrium. In particular, we have found that, during heat and matter transfer in either normal or cancer cells, the entropy density "decelerates" due to the negative value of the entropy density acceleration passing, as a function of time, from one local equilibrium state (but global non-equilibrium) to the following local equilibrium state. This "deceleration" approaches zero at large times corresponding to the global thermodynamic equilibrium.

These findings allow us to propose a reformulation of Prigogine's minimum energy dissipation principle in terms of the vanishing of the entropy density acceleration at global equilibrium and to apply it to the most representative catabolic process occurring in cells, the glucose catabolism. The results obtained for glucose catabolism can be generalized to any kind of irreversible reactions occurring in either normal or cancer cells of living systems.

2. Methods

In this section, we derive the general expressions of the entropy density acceleration for glucose catabolism resulting from the rates of entropy density calculated in [34, 35] and based on thermodynamic and statistical principles.

2.1 Entropy density acceleration for glucose catabolism

To calculate the entropy density acceleration for glucose catabolism defined as the time derivative of the rate of entropy density, namely $a(x,t) = \partial r(x,t)/\partial t$, we recall the general definition of the rate of entropy density production decomposed as $r(x,t) = r_i(x,t) + r_e(x,t)$. Here, $r_i = ds_i/dt \geq 0$ is the RIEDP with, in a compact form, $s_i = S_i/V$ (S_i is the internal entropy and V is the volume of the thermodynamic system) the internal entropy density and $r_e = ds_e/dt$ is the REEDP with, in a compact form, $s_e = S_e/V$ (S_e is the external entropy) the external entropy density. This latter quantity is often called in the literature the entropy flow or entropy flow rate or entropy production rate of the system [18, 19, 22].

However, for the sake of simplicity, we have adopted the same nomenclature of the internal contribution.

We remind that, in our previous works on the subject [34, 35], we have called REEDP the rate of entropy density contributions expressing the entropy flow rate of heat and matter reversibly exchanged from inside the cell to the intercellular environment and due to irreversible processes occurring inside the cell. This results in an increase of the rate of entropy production in the intercellular environment (external to the system represented by the cell) at the expenses of an equal decrease of the rate in the cell. This means that, if we consider the REEDP or entropy flow rate as referred to a loss of the rate of entropy density production of the cell regarded as the thermodynamic system exchanging entropy with the environment, we should take it with the negative sign as is usually done in the literature [19, 22]. However, in our framework according to which we consider the whole thermodynamic system decomposed into two subsystems, the cell and the intercellular environment, the entropy density flow rate should be interpreted as a gain for the intercellular environment and taken with the positive sign and added to the RIEDP.

Of course, when one deals with an open thermodynamic system undergoing state changes due to external driving forces also the entropy flow rate from the environment into the system should be taken into account. At a non-equilibrium steady state, the time averaged entropy change is zero due to the balancing between the entropy flow rate (either from the system to the environment or from the environment into the system) and the rate of internal entropy production [19, 22]. However, in our framework, we do not deal with driving forces external to the system and consequently with the entropy flow rate from the environment to the system since we are considering the rate of entropy produced by a single cell and consequently the entropy flow rate from the system to the environment. At global thermodynamic equilibrium, all quantities are zero.

More specifically, in our framework, $r_i(x,t) = r_{i\,Q}(x,t) + r_{i\,D}(x,t) + r_{i\,r}(x,t)$, with $r_{i\,Q}(x,t)$ the contribution due to heat flow and transfer inside the cell, $r_{i\,D}(x,t)$ the one associated to molecules diffusion and internal transport and $r_{i\,r}(x,t)$ the one due to irreversible chemical reactions occurring inside the cell. Hence, we get $a_i(x,t) = \partial r_i(x,t)/\partial t$ for the internal entropy density acceleration (IEDA) with $a_i(x,t) = a_{iQ}(x,t) + a_{iD}(x,t) + a_{ir}(x,t)$. Instead, $r_e(x,t) = r_{e\,Q}(x,t) + r_{e\,\mathrm{exch}}(x,t)$ with $r_{e\,Q}(x,t)$ ($r_{e\,\mathrm{exch}}(x,t)$) the contribution due to the heat transfer (matter exchange) from the cell to the intercellular environment. As a result, the external entropy density acceleration (EEDA), $a_e(x,t) = \partial r_e(x,t)/\partial t$ includes two contributions, $a_e(x,t) = a_{eQ}(x,t) + a_{e\,exch}(x,t)$ where $a_{eQ}(x,t) = \partial r_{eQ}(x,t)/\partial t$ ($a_{e\,\mathrm{exch}}(x,t) = \partial r_{e\,\mathrm{exch}}(x,t)/\partial dt$) is the acceleration contribution related to heat (matter) transfer between the cell and the intercellular environment. Therefore, owing to the previous definitions $a(x,t) = a_i(x,t) + a_e(x,t)$ is the total acceleration. We note, according to this framework, that the entropy density acceleration has a time and space dependence and this latter dependence is still one-dimensional as for $r(x,t) = r_i(x,t) + r_e(x,t)$.

2.2 Internal entropy density acceleration for glucose catabolism

In this subsection, we calculate the contributions to the IEDA relevant to glucose catabolism with special regard to lactic acid fermentation and respiration processes. In the calculations, we have taken into account the same assumptions made in our previous studies about the shape of the cells (cubic), the features of the heat and mass flows (unidirectional), the kind of tissue and so on [34, 35] based on direct observations for any kinds of cells (normal or cancer). The IEDA $a_{i\,Q}(x,t)$ due to heat transfer inside the cell is:

$$a_{iQ}(x,t) = \frac{\partial}{\partial t}\left[\nabla\left(\frac{1}{T(x,t)}\right)\cdot \mathbf{J}_u(x,t)\right]. \qquad (1)$$

Here, $\mathbf{J}_u = \mathbf{J}_Q + \sum_{k=1}^{N} u_k \mathbf{J}_{D\,k}$ with N the number of chemical species, $\mathbf{J}_Q$ is the irreversible heat flow, $J_{D\,k}$ is the diffusion flow of the kth chemical species, u_k is the partial molar energy and $\boldsymbol{F}_u(x,t) = \nabla(1/T(x,t))$ is the heat thermodynamic force driving $\mathbf{J}_u$ with $T(x,t)$ the temperature distribution. Instead, the IEDA due to mass diffusion and matter exchange inside the cell assumes the form:

$$a_{iD}(x,t) = -\frac{\partial}{\partial t}\left[\sum_{k=1}^{N} \nabla\left(\frac{\mu_k(x,t)}{T(x,t)}\right)\cdot \mathbf{J}_{Dk}(x,t)\right], \quad (2)$$

where the diffusion flow $\mathbf{J}_{Dk}$ is driven by the matter thermodynamic force $\mathbf{F}_k(x,t)=\nabla(\mu_k(x,t)/T(x,t))$ with μ_k the chemical potential of the kth chemical species. The entropy density acceleration generated by the chemical irreversible reactions reads:

$$a_{ir}(x,t) = \frac{\partial}{\partial t}\left[\frac{1}{T(x,t)}\sum_{j=1}^{M} A_j(x,t)v_j\right], \quad (3)$$

with $A_j(x,t) = -\sum_{k=1}^{N} \nu_{jk}\mu_k(x,t)$ the affinity of the jth chemical reaction (M is the number of chemical reactions) with ν_{jk} the stoichiometric coefficients, and $v_j = 1/V_{cell}\, d\xi_j/dt$ is the velocity of the jth reaction with $d\xi_j$ the variation of the jth degree of advancement. We now calculate the IEDA $a_{iQ}(x,t) = dr_{iQ}(x,t)/dt$ associated to the heat flow during glucose catabolism recalling the expression of $r_{iQ}(x,t)$ [35]:

$$r_{iQ}(x,t) = pK\frac{\pi^2}{L^2}\frac{\left[\sum_{n=1}^{+\infty}\left(\cos\left[(2n-1)\frac{\pi}{L}x\right]e^{-\kappa(2n-1)^2\frac{\pi^2}{L^2}t}\right)\right]^2 e^{-\frac{t}{\tau}}}{\left[\sum_{n=1}^{+\infty}\left(\frac{1}{2n-1}\sin\left[(2n-1)\frac{\pi}{L}x\right]e^{-\kappa(2n-1)^2\frac{\pi^2}{L^2}t}\right)\right]^2}. \quad (4)$$

Here, K is the thermal conductivity, L is the side of the cubic cell, κ is the thermal diffusivity in water and τ is a characteristic decay time. The coefficient p = 0.85 (0.90) expresses the frequency of occurrence of glucose catabolism in a normal (cancer) cell. According to the model, we assume that this contribution is the same for lactic acid fermentation and respiration processes. The IEDA associated to heat transfer inside the cell is:

$$a_{iQ}(x,t) = -\frac{pK\frac{\pi^2}{L^2}e^{-\frac{t}{\tau}}\sum_{n=1}^{+\infty}\left(\cos\left[(2n-1)\frac{\pi}{L}x\right]e^{-\kappa(2n-1)^2\frac{\pi^2}{L^2}t}\right)}{\left[\sum_{n=1}^{+\infty}\left(\frac{1}{2n-1}\sin\left[(2n-1)\frac{\pi}{L}x\right]e^{-\kappa(2n-1)^2\frac{\pi^2}{L^2}t}\right)\right]^2}\times$$
$$\left[\frac{1}{\tau}\left[\sum_{n=1}^{+\infty}\left(\cos\left[(2n-1)\frac{\pi}{L}x\right]e^{-\kappa(2n-1)^2\frac{\pi^2}{L^2}t}\right)\right]+\right.$$
$$\left.+2\kappa\frac{\pi^2}{L^2}\left[\frac{\left[\sum_{n=1}^{+\infty}\left((2n-1)\sin\left[(2n-1)\frac{\pi}{L}x\right]e^{-\kappa(2n-1)^2\frac{\pi^2}{L^2}t}\right)\right]\left[\sum_{n=1}^{+\infty}\left(\cos\left[(2n-1)\frac{\pi}{L}x\right]e^{-\kappa(2n-1)^2\frac{\pi^2}{L^2}t}\right)\right]}{\left[\sum_{n=1}^{+\infty}\left(\frac{1}{2n-1}\sin\left[(2n-1)\frac{\pi}{L}x\right]e^{-\kappa(2n-1)^2\frac{\pi^2}{L^2}t}\right)\right]}-\sum_{n=1}^{+\infty}\left((2n-1)^2\cos\left[(2n-1)\frac{\pi}{L}x\right]e^{-\kappa(2n-1)^2\frac{\pi^2}{L^2}t}\right)\right]\right]. \quad (5)$$

$a_{iQ}(x,t)$ includes two terms depending on the trigonometric series: the first term is inversely proportional to the characteristic decay time, while the second one is proportional to the thermal conductivity.

We now determine the IEDA $a_{iD}(x,t) = \partial r_{iD}(x,t)/\partial t$ either for respiration or fermentation process recalling the corresponding rate of entropy density [35]:

Preprints (www.preprints.org) | NOT PEER-REVIEWED | Posted: 9 November 2018 doi:10.20944/preprints201811.0233.v1

Peer-reviewed version available at Entropy 2018, 20, 929; doi:10.3390/e20120929

$$r_{i\,D\,\alpha}(x,t)=\frac{\pi^{\frac{3}{2}}}{16}\frac{1}{T_0}\frac{1}{V_{\text{cell}}}\frac{(x-L/2)e^{-\frac{t}{\tau}}}{t^{\frac{3}{2}}}\left(\sum_{k=1}^{N_\alpha}\left(u_k\frac{N_{m\,k}}{\sqrt{D_k}}e^{-\frac{(x-L/2)^2}{4D_k t}}\right)\right)\left(\frac{\left(\sum_{n=1}^{+\infty}\left(\cos\left[(2n-1)\frac{\pi}{L}x\right]e^{-\kappa(2n-1)^2\frac{\pi^2}{L^2}t}\right)e^{-|x-L/2|/L}\right)}{\left(\sum_{n=1}^{+\infty}\left(\frac{1}{2n-1}\sin\left[(2n-1)\frac{\pi}{L}x\right]e^{-\kappa(2n-1)^2\frac{\pi^2}{L^2}t}\right)\right)^2}\right). \quad (6)$$

Here, α = ferm, resp where "ferm" stands for fermentation and "resp" for respiration, T_0 is the maximum cell temperature, V_{cell} is volume of the cubic cell with L the side of the average cube, N_α is the number of chemical species in either the respiration or fermentation process, D_k is the diffusion constant of the kth chemical species, $\mu_k = u_k e^{-(|x-L/2|/L + t/\tau)}$ is the kth species chemical potential, and $N_{m\,k}$ is the number of moles of the kth chemical species. The IEDA associated to matter diffusion inside the cell either for respiration or fermentation process reads:

$$\begin{aligned}
a_{i\,D\alpha}(x,t)=&-\frac{\pi^{\frac{3}{2}}}{16}\frac{1}{T_0}\frac{1}{V_{\text{cell}}}\left(\frac{3}{2}\frac{1}{t^{\frac{5}{2}}}+\frac{1}{\tau}\frac{1}{t^{\frac{3}{2}}}\right)(x-L/2)e^{-\frac{t}{\tau}}\left(\sum_{k=1}^{N_\alpha}\left(u_k\frac{N_{m\,k}}{\sqrt{D_k}}e^{-\frac{(x-L/2)^2}{4D_k t}}\right)\right)\left(\frac{\left(\sum_{n=1}^{+\infty}\left(\cos\left[(2n-1)\frac{\pi}{L}x\right]e^{-\kappa(2n-1)^2\frac{\pi^2}{L^2}t}\right)e^{-|x-L/2|/L}\right)}{\left(\sum_{n=1}^{+\infty}\left(\frac{1}{2n-1}\sin\left[(2n-1)\frac{\pi}{L}x\right]e^{-\kappa(2n-1)^2\frac{\pi^2}{L^2}t}\right)\right)^2}\right)+\\
&+\frac{\pi^{\frac{3}{2}}}{16}\frac{1}{T_0}\frac{1}{V_{\text{cell}}}\frac{(x-L/2)^3e^{-\frac{t}{\tau}}}{t^{\frac{3}{2}}}\left(\sum_{k=1}^{N_\alpha}\left(u_k\frac{N_{m\,k}}{\sqrt{D_k}}\frac{1}{4D_k t^2}e^{-\frac{(x-L/2)^2}{4D_k t}}\right)\right)\left(\frac{\left(\sum_{n=1}^{+\infty}\left(\cos\left[(2n-1)\frac{\pi}{L}x\right]e^{-\kappa(2n-1)^2\frac{\pi^2}{L^2}t}\right)e^{-|x-L/2|/L}\right)}{\left(\sum_{n=1}^{+\infty}\left(\frac{1}{2n-1}\sin\left[(2n-1)\frac{\pi}{L}x\right]e^{-\kappa(2n-1)^2\frac{\pi^2}{L^2}t}\right)\right)^2}\right)+\\
&+\frac{\pi^{\frac{3}{2}}}{16}\frac{1}{T_0}\frac{1}{V_{\text{cell}}}\frac{(x-L/2)e^{-\frac{t}{\tau}}}{t^{\frac{3}{2}}\left[\sum_{n=1}^{+\infty}\left(\frac{1}{2n-1}\sin\left[(2n-1)\frac{\pi}{L}x\right]e^{-\kappa(2n-1)^2\frac{\pi^2}{L^2}t}\right)\right]^2}\left(\sum_{k=1}^{N_\alpha}\left(u_k\frac{N_{m\,k}}{\sqrt{D_k}}e^{-\frac{(x-L/2)^2}{4D_k t}}\right)\right)\times 2\kappa\frac{\pi^2}{L^2}\\
&\left[\frac{\left(\sum_{n=1}^{+\infty}\left((2n-1)\sin\left[(2n-1)\frac{\pi}{L}x\right]e^{-\kappa(2n-1)^2\frac{\pi^2}{L^2}t}\right)\right)\left[\sum_{n=1}^{+\infty}\left(\cos\left[(2n-1)\frac{\pi}{L}x\right]e^{-\kappa(2n-1)^2\frac{\pi^2}{L^2}t}\right)\right]}{\left[\sum_{n=1}^{+\infty}\left(\frac{1}{2n-1}\sin\left[(2n-1)\frac{\pi}{L}x\right]e^{-\kappa(2n-1)^2\frac{\pi^2}{L^2}t}\right)\right]}-\sum_{n=1}^{+\infty}\left((2n-1)^2\cos\left[(2n-1)\frac{\pi}{L}x\right]e^{-\kappa(2n-1)^2\frac{\pi^2}{L^2}t}\right)\right].
\end{aligned} \quad (7)$$

$a_{i\,D\alpha}(x,t)$ consists of three contributions each of them weighted by the trigonometric series.

Taking into account the weights w_{ferm} and w_{resp} expressing the frequency of occurrence of respiration and fermentation process in a normal and in a cancer cell (see Section 3, Results), we write the total acceleration contribution $a_{i\,D}$ due to the two metabolic pathways as:

$$a_{i\,D}(x,t)=w_{\text{resp}}\,a_{i\,D\,\text{resp}}(x,t)+w_{\text{ferm}}\,a_{i\,D\,\text{ferm}}(x,t) \quad (8)$$

Finally, we compute the IEDA $a_{i\,r}(x,t)=\partial r_{i\,r}(x,t)/\partial t$ caused by irreversible reactions occurring inside the cell during glucose catabolism via the corresponding rate expressed in the form [35]:

$$r_{i\,r\,\alpha}(x,t)=-\frac{\pi}{4}\frac{1}{T_0}\frac{1}{V_{\text{cell}}}\frac{e^{-t/\tau}\,k_{\text{kin}\,\alpha}\left(\sum_{k=1}^{N_\alpha}\nu_k u_k e^{-|x-L/2|/L}\,N_{m\ \text{Glucose}}\right)}{\sum_{n=1}^{+\infty}\left(\frac{\sin\left[(2n-1)\frac{\pi}{L}x\right]}{2n-1}e^{-\kappa(2n-1)^2\frac{\pi^2}{L^2}t}\right)}, \quad (9)$$

Preprints (www.preprints.org) | NOT PEER-REVIEWED | Posted: 9 November 2018 doi:10.20944/preprints201811.0233.v1

Peer-reviewed version available at Entropy 2018, 20, 929; doi:10.3390/e20120929

with $k_{\mathrm{kin}\,\alpha}$ the kinetic constant, ν_k stoichiometric coefficients and $N_{m\,\mathrm{Glucose}}$ the number of glucose moles (note the typo error $L/2 - x$ in the argument of the sine in Eq.(4) and Eqs.(10-11) of [35]). We get $a_{i\,r}(x,t)$ either for respiration or for lactic acid fermentation:

$$a_{i\,r\,\alpha}(x,t) = \frac{\pi}{4}\frac{1}{T_0}\frac{1}{V_{\mathrm{cell}}} e^{-t/\tau}\, k_{\mathrm{kin}\,\alpha} \sum_{k=1}^{N_\alpha} \nu_k u_k e^{-|x-L/2|/L}\, N_{m\ \mathrm{Glucose}} \times$$

$$\left[\frac{1}{\tau}\left(\sum_{n=1}^{+\infty} \left(\frac{\sin\left[(2n-1)\frac{\pi}{L}x\right]}{2n-1} e^{-\kappa(2n-1)^2\frac{\pi^2}{L^2}t} \right) \right)^{-1} - \kappa\frac{\pi^2}{L^2} \frac{\sum_{n=1}^{+\infty}\left((2n-1)\sin\left[(2n-1)\frac{\pi}{L}x\right] e^{-\kappa(2n-1)^2\frac{\pi^2}{L^2}t} \right)}{\left(\sum_{n=1}^{+\infty} \left(\frac{\sin\left[(2n-1)\frac{\pi}{L}x\right]}{2n-1} e^{-\kappa(2n-1)^2\frac{\pi^2}{L^2}t} \right) \right)^2} \right]. \quad (10)$$

We express the entropy density acceleration due to irreversible reactions during glucose catabolism in the form:

$$a_{i\,r} = w_{\mathrm{resp}}\, a_{i\,r\,\mathrm{resp}} + w_{\mathrm{ferm}}\, a_{i\,r\,\mathrm{ferm}} \quad (11)$$

with different weights for respiration and fermentation process (See Section 3, Results).

2.3 External entropy density acceleration for glucose catabolism

In this subsection, we calculate the external entropy density acceleration (EEDA) starting from the corresponding REEDP calculated in [34,35]. The EEDA $a_e(x,t) = \partial r_e(x,t)/\partial t$ includes two contributions, namely $a_e(x,t) = a_{e\,Q}(x,t) + a_{e\,\mathrm{exch}}(x,t)$. Here, $a_{e\,Q}(x,t) = \partial r_{e\,Q}(x,t)/\partial t$ ($a_{e\,\mathrm{exch}}(x,t) = \partial r_{e\,exch}(x,t)/\partial t$) is the acceleration contribution related to heat (matter) transfer between the cell and the intercellular environment. The general expression for $a_{e\,Q}(x,t)$ reads:

$$a_{e\,Q}(x,t) = \frac{\partial}{\partial t}\left(\frac{1}{T_{\mathrm{ic}}(x,t)} \frac{1}{\mathrm{V}_{\mathrm{cell}}} \frac{dQ}{dt} \right). \quad (12)$$

where T_{ic} is the intercellular temperature and dQ/dt is the time derivative of the heat. Instead, the general expression for $a_{e\,\mathrm{exch}}$ takes the form:

$$a_{e\,\mathrm{exch}}(x,t) = -\frac{\partial}{\partial t}\left(\frac{1}{T_{\mathrm{ic}}(x,t)} \sum_{k=1}^{N_{\mathrm{pr}}} \mu_k(x,t) \frac{d_e N_{m\,k}}{dt} \right), \quad (13)$$

where $N_{m\,k}$ is the number of moles of the kth product of reaction.

To calculate the $a_{e\,Q}$ contribution to EEDA, we recall the corresponding REEDP for respiration and fermentation process [35]:

$$r_{eQ\ \alpha}(x,t) = \frac{1}{\mathrm{V}_{\mathrm{cell}}} \frac{3}{8} k_B N_A N_{m\ \mathrm{pr}\,\alpha} \left[\frac{1}{\kappa}\frac{(x-L)^2}{t^2} - \frac{2}{t} \right], \quad (14)$$

where, $k_B = 1.3805 \times 10^{-23}$ J/K is the Boltzmann constant, $N_{\mathrm{m\ pr\ resp}}$ ($N_{m\ \mathrm{pr\ ferm}}$) is the number of moles of the products in respiration (fermentation) process. Note the contribution proportional to $1/t$ on the second member that breaks the time reversal symmetry [34] as occurs for the other rate contributions. In principle, at small distances from the border of the cell (for small x) the term proportional to $1/t$ is greater than the term proportional to $1/t^2$ resulting in a negative $r_{e\,Q}$ for the typical intercellular size. However, in our model, we have set ourselves under the hypothesis of large x and small t (1000 μs << 1 s) neglecting the term proportional to $1/t$ even close to the cell border yielding:

$$r_{eQ\alpha}(x,t) \simeq \frac{1}{V_{cell}} \frac{3}{8} k_B N_A N_m \, \mathrm{pr}\alpha \frac{1}{\kappa} \frac{(x-L)^2}{t^2}. \quad (15)$$

This assumption has allowed us to get a positive r_{eQ} for any x outside the cell and any t. This means that the entropy outside the cell increases because of the heat released by the irreversible reactions occurring inside the cell but this increase leads to a decrease of the rate of entropy of the cell because heat is removed from the cell. Hence, the EEDA $a_{eQ}(x,t)$ takes the simple form:

$$a_{eQ\alpha}(x,t) \simeq -\frac{1}{V_{cell}} \frac{3}{8} k_B \frac{N_A N_m \, \mathrm{pr}\alpha}{\kappa} \frac{(x-L)^2}{t^3}. \quad (16)$$

The total entropy density acceleration reads:

$$a_{eQ} = w_{resp} a_{eQ\,resp} + w_{ferm} a_{eQ\,ferm}, \quad (17)$$

with different weights for a normal and a cancer cell (See Section 3, Results).

Let us now calculate the last entropy acceleration contribution caused by irreversible exchange of matter. To do this we recall the REEDP due to irreversible exchange of matter with the intercellular environment during glucose catabolism [35]:

$$r_{e\,exch\,\alpha}(x,t) = -\frac{1}{T_0} \frac{1}{V_{cell}} \frac{\sqrt{4\pi\kappa t}}{x_0} e^{\frac{(x-L)^2}{4\kappa t}} e^{-t/\tau} \sum_{k=1}^{N_{pr}\alpha} u_k \, e^{-|x-L/2|/L} \frac{d_e N_m \, k\alpha}{d\tau_\beta}. \quad (18)$$

Here, $x_0 = 10$ µm is a characteristic length having the size of a normal cell, $d\tau_\beta$ (β=1,2 with 1 referred to respiration and 2 to fermentation) is a characteristic time such that $1/d\tau_1$ ($1/d\tau_1$) is 10^{-5} s^{-1} (10^{-4} s^{-1}) of the order of k_{kin}, $N_{pr\,resp}$ ($N_{pr\,ferm}$) is the number of products of the respiration (fermentation) process. Also this matter contribution has a positive contribution if referred to the intercellular environment but it would be taken as negative if referred to the cell because matter exchange leads to a removal of the products of irreversible reactions from the cell.

The EEDA $a_{e\,exch\,\alpha}(x,t) = dr_{e\,exch}(x,t)/dt$ resulting from irreversible exchange of matter with the intercellular environment turns out to be:

$$a_{e\,exch\,\alpha}(x,t) = \frac{1}{T_0} \frac{1}{V_{cell}} \frac{1}{x_0} e^{\frac{(x-L)^2}{4\kappa t}} e^{-t/\tau} \left(\frac{1}{\tau} \sqrt{4\pi\kappa t} - \sqrt{\frac{\pi\kappa}{t}} + \sqrt{\frac{\pi}{\kappa}} \frac{(x-L)^2}{2t^{\frac{3}{2}}} \right) \sum_{k=1}^{N_{pr}\alpha} u_k \, e^{-|x-L/2|/L} \frac{d_e N_{m\,k\alpha}}{d\tau_\beta} \quad (19)$$

We calculate the entropy acceleration related to exchange of matter with the intercellular environment as:

$$a_{e\,exch} = w_{ferm} \, a_{e\,exch\,ferm} + w_{resp} \, a_{e\,exch\,resp} \quad (20)$$

with different weights for a normal and a cancer cell (See Section 3, Results).

3. Results

In this section, we compute the IEDA and the EEDA generated by inner and outer heat and matter transfer either a normal or a cancer cell during glucose catabolism by performing the numerical derivatives of the corresponding RIEDP and REEDP whose analytical expressions were given in Section 2. Indeed, the analytical computation of the IEDA would lead to some convergence problems

due to their complex analytical expressions involving several trigonometric series depending on the index n.

We first determine the entropy density acceleration taking into account the occurrence of both respiration and fermentation metabolic pathways occurring with different weights in a normal and cancer cell. Then, we single out the entropy density acceleration due to either respiration or lactic acid fermentation in a representative cell having the size of a normal cell. Cell respiration consists of three steps, viz. glycolysis, Krebs cycle and oxidative phosphorylation involving glucose and oxygen, $C_6H_{12}O_6 + 6O_2 \rightarrow 6\ CO_2 + 6\ H_2O$ and leading to the formation of carbon dioxide (CO_2) and water (H_2O). Instead, fermentation process consists only of glycolytic step, $C_6H_{12}O_6 \rightarrow 2\ C_3H_5O_3^- + 2\ H^+$ and leads to the formation of lactic acid ions ($C_3H_5O_3^-$) and hydrogen ions (H^+).

For consistency, in the numerical calculations of acceleration densities, we have employed the same numerical parameters used in our previous studies [34, 35]. In particular, we have taken an average size L = 10 μm (L = 20 μm) for the normal cell (cancer cell) taking as reference the breast epithelium and assuming, without loss of generality, a cubic shape and an average size of the intercellular space about 0.2-0.3 μm (1.5 μm) between two adjacent normal (cancer) cells. For all acceleration entropy densities, we have chosen $\tau \approx 10^{-4}$ s as a typical cell decaying time. We have taken as weights for respiration (fermentation) process w_{resp}=0.8 (w_{ferm}=0.2) in a normal cell and w_{resp}=0.1 (w_{ferm}=0.9) in a cancer cell. We have also used for both normal and cancer cells the following parameters:
thermal conductivity K = 0.600 J/ (m s K), thermal diffusivity in water $\kappa_{H20} = 0.143 \times 10^{-6}$ m^2/s, diffusion constants at standard conditions: $D_{C6H12O6} = 6.73 \times 10^{-10}$ m^{2}s^{-1}, $D_{O2} = 21.00 \times 10^{-10}$ m^{2}s^{-1}, $D_{CO2} = 19.20$ kJ/mole $\times 10^{-10}$ m^{2}s^{-1}, $D_{H2O} = 21.00 \times 10^{-10}$ m^{2}s^{-1}, $D_{C3H5O3-} = 9.00 \times 10^{-10}$ m^{2}s^{-1} and $D_{H+} = 45.00 \times 10^{-10}$ m^{2}s^{-1} in aqueous solution. Finally, we have employed the partial molar energies or chemical potentials at t = 0 and $x = L/2$ and, at standard conditions: $\mu_{C6H12O6}$ = -917.44 kJ/mole, μ_{O2} = 16.44 kJ/mole, μ_{CO2} = -385.99 kJ/mole, μ_{H2O} = -237.18 kJ/mole, $\mu_{C3H5O3-}$ = -516.72 kJ/mole where $C_3H_5O_3^-$ is the lactate ion and μ_{H+} = 0 kJ/mole in aqueous solution.

In particular, for the calculation of $a_{i\ Q}$ we have taken as frequency of occurrence of glucose catabolism the value p = 0.85 (0.90) for normal (cancer) cells, while for the calculation of a_{ir} we have taken as values of the pathway kinetic constants $k_{kin}^{resp} = 10^{-5}$ s^{-1} and $k_{kin}^{ferm} = 10^{-4}$ s^{-1}, and $N_{m\ Glucose}$ = 1 as a reference concentration.

3.1 Entropy density accelerations for normal and cancer cells: numerical calculations

In this study, we show the numerical calculations of the IEDA and EEDA for normal and cancer breast cells. For every term, we represent the corresponding acceleration entropy density as a function of the spatial coordinate x and of the time coordinate t. We choose for all accelerations a time interval Δt =1000 μs, a Δt typical of most biological processes [35].

Note that in the main panels we plot all the entropy density accelerations in the time interval 100 ÷1000 μs with the exception of $a_{e\ Q}$. Indeed, in the first instants of time (0÷100 μs), some terms of the entropy density acceleration are positive as depicted in the insets and, due to the appreciable magnitude, this would mask the leading negative trend of the accelerations in the time interval 100÷1000 μs. The positive trend of most of the accelerations during the first instants of time is not surprising and is due to the initial increasing behavior of the corresponding rates. Of course, this behaviour is only secondary to the leading and most important negative trend characterizing all the entropy density accelerations.

3.1 Internal entropy density acceleration: numerical calculations

In this section, we show the spatial and time dependence of the IEDA obtained from the previous formalism.

In Figure 1, we display the IEDA space and time profiles for both normal and cancer cells resulting from the heat and matter transfer inside cells and from the irreversible chemical reactions in the

representative time interval 100 ÷1000 s. The common features are: 1) the negative value of the IEDA corresponding to a "deceleration" and 2) their increase with increasing time. Figure 1(a) and (b) show a_{iQ} calculated according to Equation (5) for a normal and a cancer cell, respectively. For both kinds of cells, a_{iQ} dramatically increases with time close to the cell borders, while in the region close to the cell center exhibits a weak increase and an almost flat profile especially in the cancer cell. For $t > 500$ μs the spatial and time profile of a_{iQ} is rather flat passing from the borders to the cell center and approaches zero with increasing time.

In contrast, a_{iD} obtained from Equation (7) and Equation (8) exhibits a strong increase in the central region of the cell for the initial instants of time in both kinds of cells tending to zero for increasing time in the whole cell and exhibiting a flat profile (Figure 2(c) and (d)). Note the narrower shape of a_{iD} in a cancer cell with respect to that in a normal cell, its higher rate of increase at the initial instants of time and a minimum value that is two orders of magnitude less than that of a normal cell. We attribute the general trend to the prevalence of the fermentation process in the cancer cell, while the lesser deep minimum is related to the bigger size of the cancer cell.

Finally, in Figure 1(e) and (f) we depict a_{ir} computed according to Equation (10) and Equation (11). a_{ir} uniformly increases throughout the whole cell with increasing time but the rate of increase is much higher in a normal cell with respect to a cancer cell. Indeed, for a normal cell a_{ir} approaches values close to zero for t less than 500 μs, while for a cancer cell this occurs for t more than 500 μs. This slower tendency towards zero in a cancer cell could be due to the prevalence of lactic acid fermentation. Moreover, the minimum value of a_{ir} in a cancer cell is three orders of magnitude less than that of a normal cell and this is in part due to the bigger size of the cancer cell.

In the insets of Fig.1, we have plotted the IEDA for the initial instants of time (interval 0 ÷ 100 μs). Interestingly, every contribution is positive with the exception of a_{ir} for a normal cell that is negative throughout the whole cell and a_{ir} for a cancer cell that is negative especially in the central part of the cell. In particular, a_{iQ} for both a normal and a cancer cell and a_{ir} for a cancer cell exhibit positive values close to the cell borders, while a_{iD} exhibits remarkable positive values close to the cell centre with some differences as a function of time between a normal and a cancer cell. The positive trend of these contributions reflects the increase of the corresponding rates at the first instants of time. The positive behaviour of a_{ir} in a cancer cell close to the cell borders could be due to the prevalence of the fermentation process with respect to the respiration process.

Preprints (www.preprints.org) | NOT PEER-REVIEWED | Posted: 9 November 2018 doi:10.20944/preprints201811.0233.v1

Peer-reviewed version available at Entropy 2018, 20, 929; doi:10.3390/e20120929

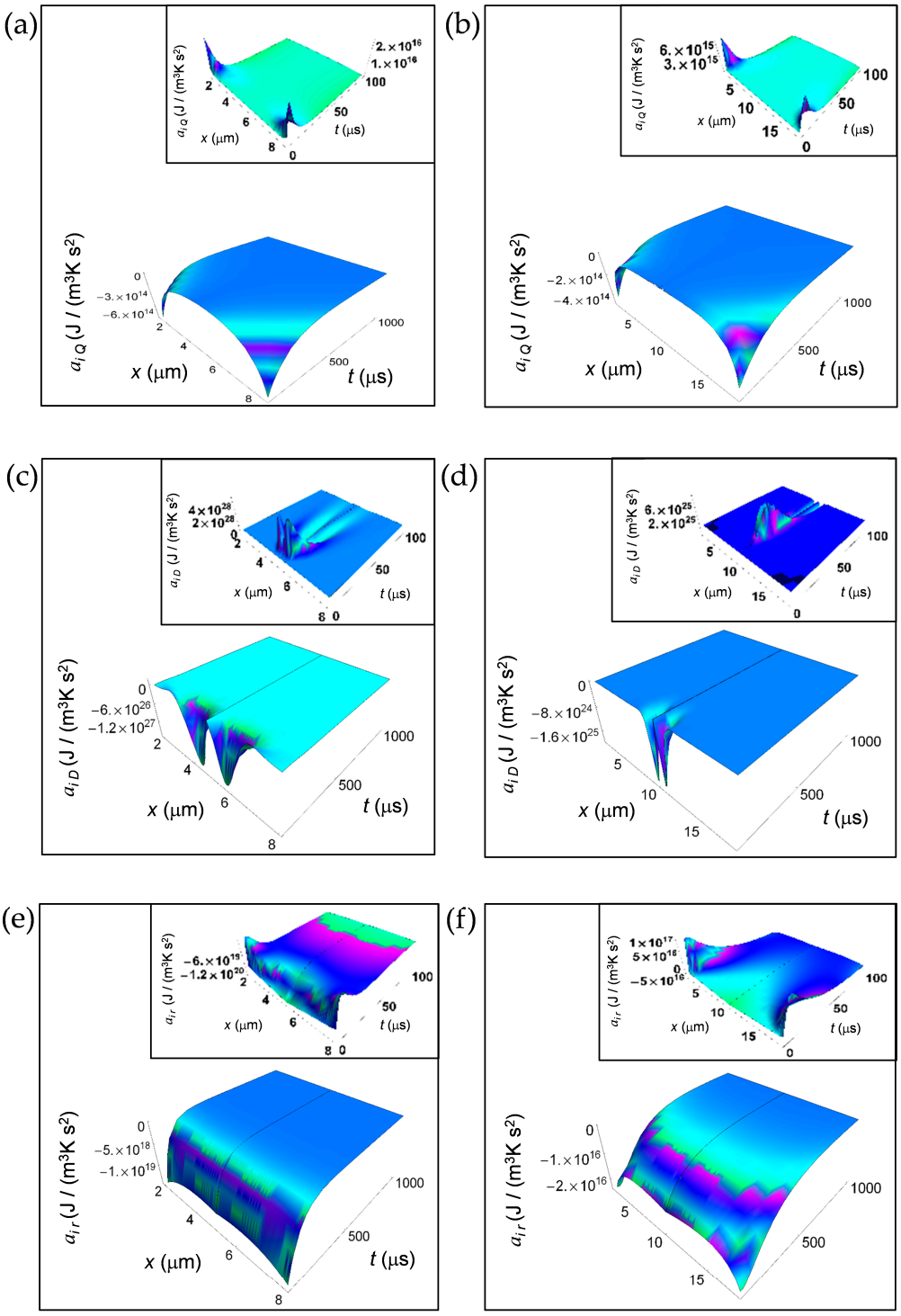

Figure 1. IEDA generated by heat, matter and irreversible reactions during glucose catabolism for a time interval of 1000 μs. (a) Calculated a_{iQ} for a normal cell. Inset: calculated a_{iQ} for a normal cell in the interval 0 ÷ 100 μs. (b) As in panel (a) but for a cancer cell. (c) Calculated a_{iD} for a normal cell. Inset: calculated a_{iD} for a normal cell in the interval 0 ÷ 100 μs. (d) As in panel (c) but for a cancer cell. (e) Calculated a_{ir} for a normal cell. . Inset: calculated a_{ir} for a normal cell in the interval 0 ÷ 100 μs. (f) As in panel (e) but for a cancer cell.

3.2 External entropy density acceleration: numerical calculations

In this section, we show the spatial and time dependence of the EEDA obtained from the previous formalism.

Figure 2 shows the EEDA spatial and time profiles generated by heat and matter transfer from the cell to the intercellular environment. In Figure 2(a) and (b) we depict the calculated $a_{e\,Q}$ for a normal and a cancer cell, respectively calculated according to Equation (16) and Equation (17). For this entropy density acceleration, we have performed the numerical calculations taking the interval of time 0 -1000 μs because $a_{e\,Q}$, unlike the other contributions, does not exhibit a positive trend during the interval of time 0 -100 μs.

The more one gets away from the border of the cell, the more the trend of entropy density acceleration becomes sharp exhibiting a strong increase during the initial instants of time that is very similar both in a normal and in a cancer cell. After the initial instants of time, the spatial and time profile of $a_{e\,Q}$ becomes flat tending to vanish with increasing t.

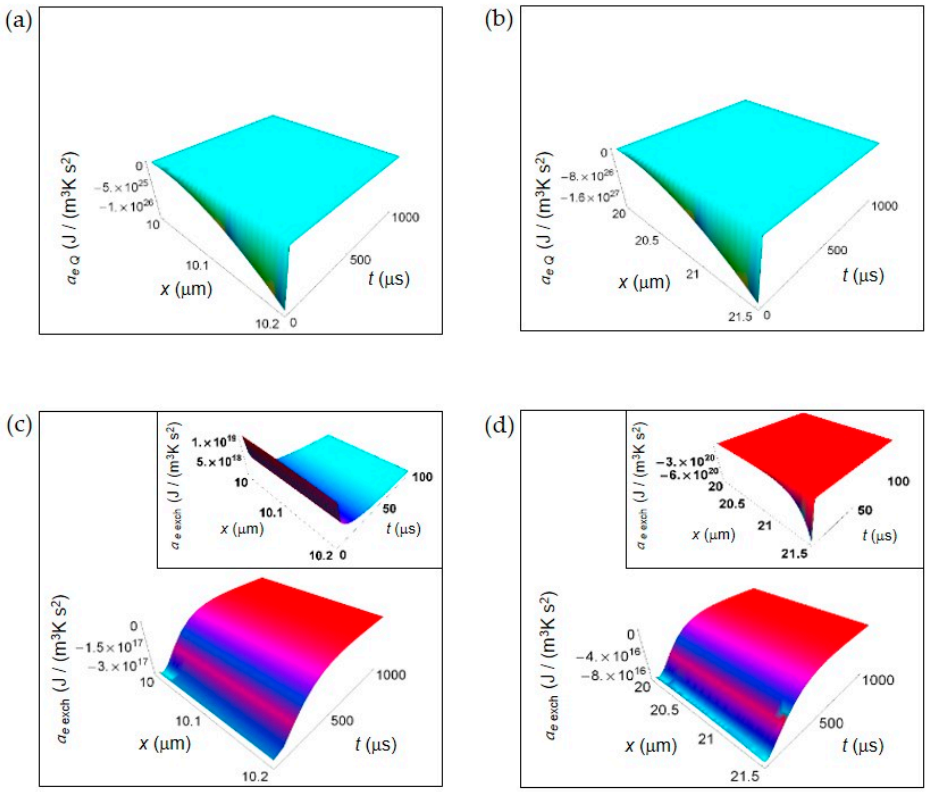

Figure 2. EEDA associated to heat and matter transfer between the cell and the intercellular envinronment. (a) Calculated $a_{e\,Q}$ for a normal cell. (b) As in (a), but for a cancer cell. (c) Calculated $a_{e\,exch}$ for a normal cell. Inset: calculated $a_{e\,exch}$ for a normal cell in the interval 0 ÷ 100 μs. (d) As in (c), but for a cancer cell.

In Fig.2(c) and (d) are displayed the $a_{e\,exch}$ for a normal and a cancer cell calculated according to Equation (19) and Equation (20). The general trend is a uniform increase throughout the intercellular environment during the first instants of time. A sharper increase of $a_{e\,exch}$ characterizes the cancer cell because of the prevalence of the fermentation process. However, on average the absolute value of $a_{e\,exch}$ for a cancer cell is less than for a normal cell. For t larger than 500 μs, in both cases $a_{e\,exch}$ approaches zero with increasing time. In the insets of Figure 2(c) and Figure 2(d), $a_{e\,exch}$ plotted in the first instants of time (interval 0 ÷ 100 μs) show an opposite behaviour taking positive values for a normal cell, and negative values for a cancer cell. This is not surprising and may be attributed to the different size of the cells

Figure 3 shows the IEDA spatial and time profiles (time interval 100 ÷1000 μs) due to matter transfer under the hypothesis of either fermentation or respiration metabolic pathways inside a

Preprints (www.preprints.org) | NOT PEER-REVIEWED | Posted: 9 November 2018 doi:10.20944/preprints201811.0233.v1

Peer-reviewed version available at Entropy 2018, 20, 929; doi:10.3390/e20120929

representative cell having the size of a normal cell. In Figure 3 (a) and (b), we depict $a_{i\,D}$ resulting from lactic acid fermentation and respiration processes, respectively and calculated by means of Equation(7). In the first instants of time, there is a strong rate of increase of $a_{i\,D}$ in the central region of the cell for both processes where $a_{i\,D}$ is strongly negative. However, there is a broader spatial and time dependence of $a_{i\,D}$ for respiration leading to a more extended region of the cell having negative $a_{i\,D}$ for small t. In addition, also the minimum of $a_{i\,D}$ symmetric on the left and on the right of the centre of the cell is deeper for respiration. For both processes with increasing time $a_{i\,D}$ becomes flat and approaches zero. Figure 3(c) and (d) display the corresponding $a_{i\,r}$ of the metabolic pathways calculated via Equation (10). Unlike $a_{i\,D}$, there are not relevant differences in the spatial trends of $a_{i\,r}$ in the two processes that are uniformly negative throughout the cell even though the minimum for fermentation is much deeper than that for respiration. This trend is in part due to the kinetic constant k_{kin}^{resp} that is one order of magnitude less than k_{kin}^{ferm}.

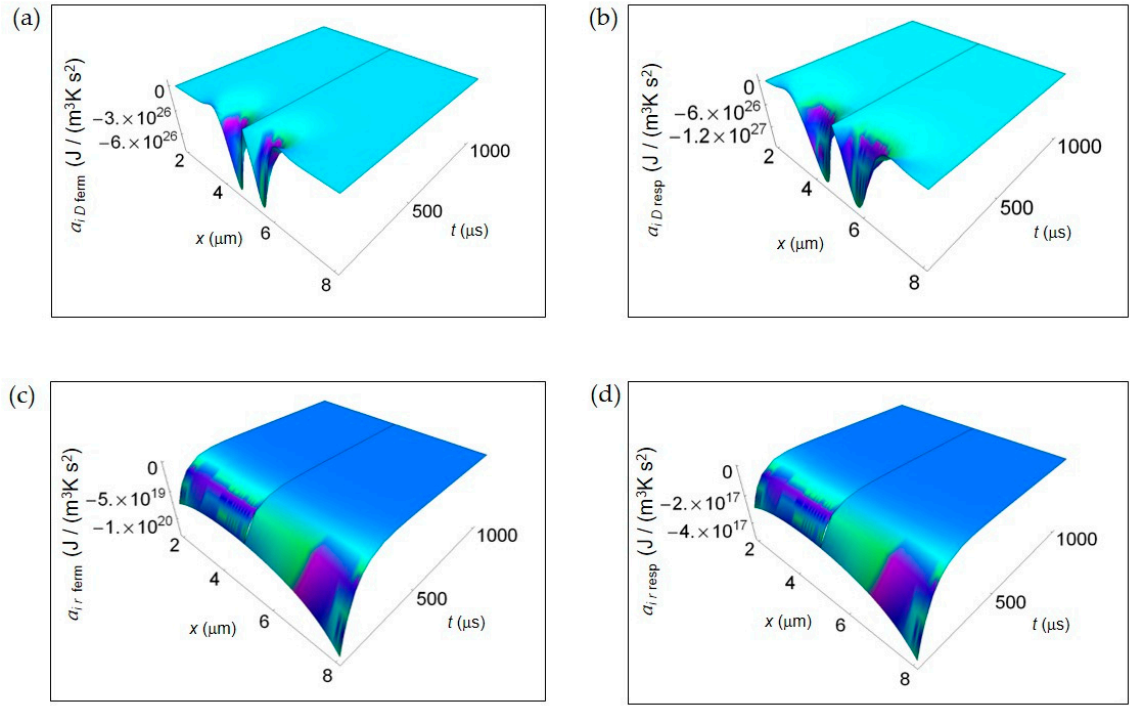

Figure 3. IEDA associated to matter transfer inside the cell for lactic acid fermentation and respiration. A representative cell having the size of a normal cell is depicted. (a) Calculated $a_{i\,D}$ for fermentation process. (b) As in (a), but for respiration process. (c) Calculated $a_{i\,r}$ for fermentation process. (d) As in (c), but for respiration process.

In Figure 4, we represent the EEDA spatial and time profiles (time interval 100 ÷1000 μs) due to heat transfer and mass exchange from inside the cell to the intercellular environment for the two metabolic pathways. Figure 4(a) and (b) show $a_{e\,Q}$ for lactic acid fermentation and respiration, respectively calculated using Equation (16). In both cases $a_{e\,Q}$ exhibits a deep negative minimum the more the distance from the cell border that is of the same order of magnitude but more pronounced for respiration process. The rate of increase of $a_{e\,Q}$ with increasing time is the same approaching zero uniformly in space still at the initial instants of time. In Figure 4(c) (Figure 4(d)) $a_{e\,exch}$ computed according to Equation (18) is displayed for lactic acid fermentation (respiration). Like for $a_{e\,Q}$ the order of magnitude of the negative minimum is the same but, with increasing the distance from the cell border, the trend of $a_{e\,exch}$ remains uniform for both processes. More specifically, the rate of increase of $a_{e\,exch}$ is slightly higher for lactic acid fermentation even though, at $t > 500$ μs, $a_{e\,exch}$ becomes flat and tends to vanish for both processes.

Preprints (www.preprints.org) | NOT PEER-REVIEWED | Posted: 9 November 2018 doi:10.20944/preprints201811.0233.v1

Peer-reviewed version available at Entropy 2018, 20, 929; doi:10.3390/e20120929

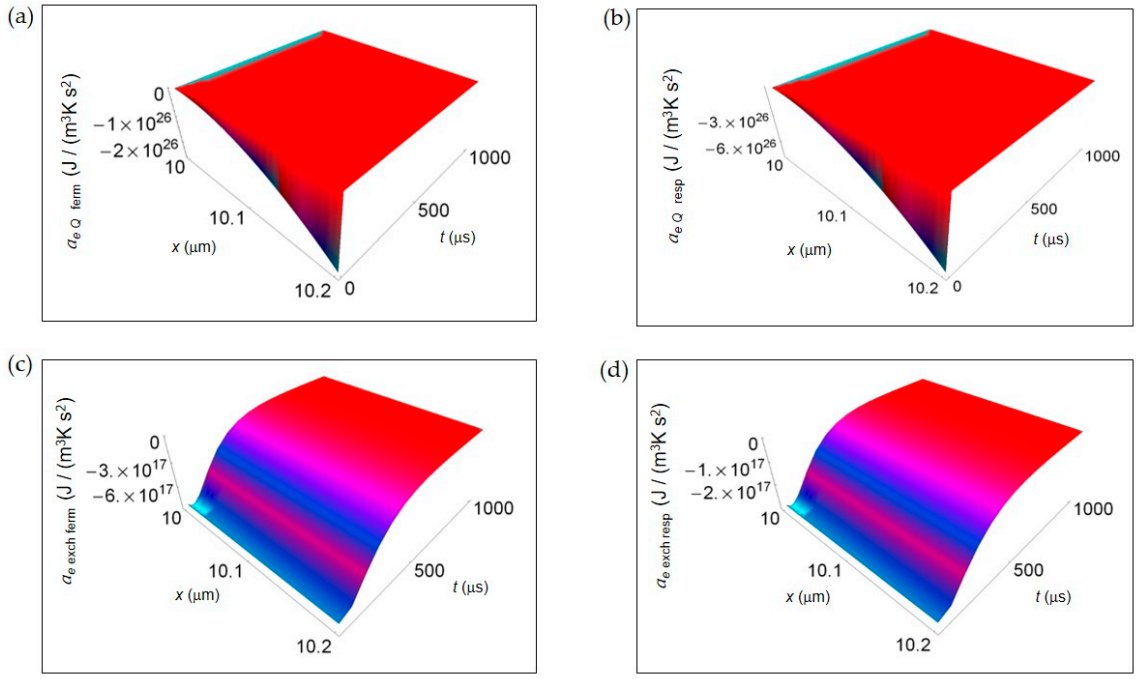

Figure 4. EEDA associated to heat and matter transfer from inside the cell to the intercellular environment for lactic acid fermentation and respiration. A representative cell having the size of a normal cell is depicted. (a) Calculated $a_{e\,Q}$ for fermentation process. (b) As in (a), but for respiration process. (c) Calculated $a_{e\ exch}$ for fermentation process. (d) As in (a), but for respiration process.

In Figure 3 and Figure 4, we have not shown the trend of the IEDA due to matter transfer for the two main metabolic pathways during the initial time interval 0÷100 μs. Indeed, the main features of the entropy accelerations in this time interval are very similar to those exhibited for the real glucose catabolism process where there is a mixture of lactic acid fermentation and respiration.

Discussion

The classical thermodynamic description of glucose catabolism in normal and cancer cells and of fermentation and respiration processes by using the concept of entropy density acceleration allows us to add further important results on irreversible processes in living systems [34, 35]. In particular, the analysis extended to the second order in time has strengthened the results obtained in relation to Prigogine's minimum dissipation principle formulated for living systems in terms of the rate of entropy density. This has been accomplished transferring from mechanics to statistical thermodynamics the concept of "motion" and of acceleration of entropy. We have found that the "motion" characterizing the entropy density in minimum living systems represented by either normal or cancer cells and associated to glucose catabolism and, more specifically, to lactic acid fermentation and respiration processes can be described as a decelerated "motion" because of the negative IEDA and EEDA. Note, however, the exceptions represented by the trends of $a_{i\,Q}$, $a_{i\,D}$ and $a_{e\ exch}$ for both kinds of cells and $a_{i\,r}$ for a cancer cell during the first instants of time (interval 0-100 μs) where the entropy density accelerations are positive because of the peculiar time behaviour of the terms contributing to these accelerations for small t.

From the inspection of the trend of the out-of-equilibrium IEDA and EEDA, the entropy density acceleration has a remarkable magnitude because of the strong variation as a function of time of the corresponding rates [35]. As a further confirmation of our previous findings where it was found that the entropy gain per unit time was higher during lactic acid fermentation, the total entropy acceleration during lactic acid fermentation has a more pronounced minimum if compared to the corresponding one exhibited by the total acceleration during respiration. We attribute this behaviour

Peer-reviewed version available at Entropy 2018, 20, 929; doi:10.3390/e20120929

especially to the $a_{i\,r}$ contribution that, for the same cell size taken as reference, is a few orders of magnitude (see Figure 3 (c)) larger for lactic acid fermentation process than for respiration and also to the $a_{e\,\mathrm{exch}}$ contribution that exhibits a minimum about three times larger for lactic acid fermentation. Indeed, due to the bigger volume of a cancer cell (on average 8 times the one of the normal cell) and to the spatial dependence along x that in a cancer cell is twice the one of the normal cell, $a_{i\,r}$ and $a_{e\,\mathrm{exch}}$ shown in Figure 1(f) and Figure 2(d), respectively look only apparently of smaller magnitude in a cancer cell than in a normal cell. This finding reiterates the concept that cancer cells, where lactic acid fermentation prevails, are characterized by a higher entropy gain per unit time (rate of entropy) as found in [35] and, therefore, by a bigger negative entropy acceleration during the initial instants of time.

Very close to the global thermodynamic equilibrium, Prigogine's minimum energy dissipation principle is fulfilled and can be reformulated in terms of the minimization of the entropy density acceleration for large times. More specifically, the total entropy density acceleration $a(x,t)$ exhibits a rather out-of-equilibrium deep negative minimum, reduces its magnitude passing through negative values with increasing time and, at the global thermodynamic equilibrium, equals zero independently of the nature of the cell and of the metabolic pathway. Straightforwardly, from the space and time profile of the entropy density acceleration, the spatial profile of the energy dissipation function could be obtained, showing that it tends to a minimum value (zero) approaching global thermodynamic equilibrium.

We believe that the study of the space and time behaviour of this thermodynamic quantity could enable to understand more in depth the entropy exchanges in minimum living systems and to give more details on the out-of-equilibrium thermodynamics of lactic acid fermentation and respiration. The notion of entropy density acceleration is easily generalizable to other irreversible reactions occurring in cells and this would give a comprehensive characterization of the thermodynamics of all irreversible processes.

Finally, the theoretical findings of this work could pave the way to further experiments. Anyway, the results of the theoretical analysis carried out in this work with special regard to the thermodynamic characterization of fermentation and respiration metabolic pathways are consistent with several works in the literature [13, 15]. Presently, exchanges of heat and matter in living systems are measured by using the direct calorimetric and the modern omics techniques with special emphasis to the measurement of the entropy production in normal cells, cancer cells, stem cells and cancer stem cells.

5. Conclusions

In conclusion, the thermodynamics of minimum living systems with special regard to irreversible reactions occurring during glucose catabolism has been theoretically studied via the introduction and the detailed calculation of a quantity directly derived from the well-known rate of entropy density production that we named entropy density acceleration. This latter is defined as the time derivative of the rate of entropy density production and expresses the time behaviour at the second order of the entropy generated inside and outside the cell. This was accomplished basing on the idea that a mechanical concept like the one of acceleration may be transferred from mechanics to thermodynamics enabling to understand better the entropy generation caused by heat and matter transfer in turn due to irreversible processes in normal and cancer cells. Owing to this, the well-known Prigogine's minimum energy dissipation principle at global thermodynamic equilibrium is reformulated in terms of the vanishing of the entropy density acceleration. The advantage of this approach is that it is possible to determine quantitatively the curvature of the rate of entropy density out-of-equilibrium not only for glucose catabolism where lactic acid fermentation and respiration processes take place in different percentages in normal and cancer cells but also focusing on the specific metabolic pathway. This has allowed to confirm that lactic acid fermentation is characterized by a deepest minimum entropy density acceleration and thus by a bigger variation of it as it approaches the global thermodynamic equilibrium.

The findings of this work could open the route towards other investigations focusing on the statistical thermodynamic description of glucose catabolism in human cells with special regard to entropy generation, entropy balance and entropy exchange and how these phenomena are related to the entropy density acceleration.

Acknowledgments: This work was partially supported by National Group of Mathematical Physics (GNFM-INdAM). The authors are grateful to Fabio Borziani for helpful discussion and kind support in this research activity.

Author Contributions: Roberto Zivieri performed the analytical and numerical calculations with inputs from Nicola Pacini. Both authors contributed to the research work, wrote, read and approved the manuscript.

Conflicts of Interest: The authors declare no conflicts of interest.

References

1. Prigogine, I.; Wiame, J.M. (1946) Biologie et thermodynamique des phenomenes irrversibles. *Experientia* **1946**, *2*, 451- 453, doi: 10.1007/BF02153597.
2. Luisi, P.L. The minimal autopoietic unit. *Orig. Life Evol. Biosph.* **2014,** 44, 335–338, doi: 10.1007/s11084-014-9388-z.
3. Keller, M.A.; Turchyn, A.V.; Ralser, M. Non-enzymatic glycolysis and pentose phosphate pathway-like reactions in a plausible Archean ocean. *Mol. Syst. Biol.* **2014,** 10, 725, 10.1002/msb.20145228.
4. Prigogine, I; Nicolis, G. Biological order, structure and instabilities. *Quarterly Reviews of Biophysics* **1971**, *4*, 107-148, doi: 10.1017/S0033583500000615.
5. Fermi, *E. Thermodynamics;* Prentice Hall, USA, 1937.
6. Hsu, C.F.; Wei, S.-Y.; Huang, H.-P.; Hsu, L.; Chi, S.; Peng, C.-K. Entropy of Entropy: Measurement of Dynamical Complexity for Biological Systems. *Entropy* **2017**, 19, 550. doi: 10.3390/e19100550.
7. Zotin, A.A. (2014) Why linear thermodynamics does describe change of entropy production in living systems? *Natural Science* **2014**, *6*, 495-502, doi: 10.4236/ns.2014.67048.
8. Zotin, A.A.; Zotin, A.I. Phenomenological theory of ontogenesis. *Int. J. Dev. Biol.* **1997**, 41**,** 917–921.
9. Warburg, O.; Wind, F.; Negelein, E. The metabolism of tumors in the body. *J. Gen. Physiol*. **1927**, 8, 519–530, doi: 10.1085/jgp.8.6.519.
10. Warburg, O. On respiratory impairment in cancer cells. *Science* **1956,** 124, 269–270.
11. Pacini, N.; Borziani, F. Cancer stem cell theory and the Warburg effect, two sides of the same coin? *Int. J. Mol. Sci.* **2014**, 15, 8893–8930, doi: 10.3390/ijms15058893.
12. Pacini, N.; Borziani, F. Oncostatic-cytoprotective effect of melatonin and other bioactive molecules: a common target in mitochondrial respiration. *Int. J. Mol. Sci.* **2016**, 17**,** 344, doi: 10.3390/ijms17030341.
13. Wong, C. C.; Qian, Y.; Yu, J. Interplay between epigenetics and metabolism in oncogenesis: mechanisms and therapeutic approaches. *Oncogene* **2017**, 36, 3359-3374, doi: 10.1038/onc.2016.485.
14. Peng, M.; Yin, N.; Chhangawala, S; Xu, K; Leslie, C.S.; Li Mo. Aerobic glycolysis promotes T helper 1 cell differentiation through an epigenetic mechanism. *Science* **2016**, 354, 481–484, doi: 10.1126/science.aaf6284.
15. Moussaieff, A.; Rouleau, M; Kitsberg, D; Cohen, M; Levy, G; Barasch, D; Nemirovski, A; Shen-Orr, S; Laevsky, I; Amit, M; Bomze, D; Elena-Herrmann, B; Scherf, T; Nissim-Rafinia, M; Kempa, S; Itskovitz-Eldor, J; Meshorer, E; Aberdam, D; Nahmias, Y. Glycolysis-mediated changes in acetyl-CoA and histone acetylation control the early differentiation of embryonic stem cells. *Cell Metab.* **2015**, 21, 392–402, doi: 10.1016/j.cmet.2015.02.002.
16. Vilar, J.M.G. Entropy of leukemia on multidimensional morphological and molecular landscapes. *Phys. Rev. X* **2014**, 4, 021038, doi: 10.1103/PhysRevX.4.021038.
17. Ridden, S.J.; Chang, H.H.; Zygalakis, K.C.; MacArthur, B.D. Entropy, ergodicity, and stem cell multipotency. *Phys. Rev. Lett.* **2015**, 115, 208103, doi: 10.1103/PhysRevLett.115.208103.

18. Kondepudi, D.; Prigogine, I. *Modern Thermodynamics: From Heat Engines to Dissipative Structures*; Wiley: New York, NY, USA, 2015.
19. Endres, R. G. Entropy production selects nonequilibrium states in multistable systems. *Sci. Rep.* **2017**, 7, 14437, doi: 10.1038/s41598-017-14485-8.
20. Ritchie, M. E. Reaction and diffusion thermodynamics explains optimal temperatures of biochemical reactions. *Sci. Rep.* **2018**, 8, 11105, doi: 10.1038/s41598-018-28833-9.
21. Tomé, T.; De Oliveira, M. J. Stochastic mechanics of nonequilibrium systems. *Braz. J. Phys.* **1997**, 27, 525, doi: 10.1590/S0103-97331997000400016**.**
22. Landi, G. T.; Tomé, T; de Oliveira, M. J. Entropy production in linear Langevin systems. *J. Phys. A: Math. Theor.* **2013**, *46*, 395001, doi: 10.1088/1751-8113/46/39/395001.
23. Tomé, T. Entropy production in nonequilibrium systems described by a Fokker-Planck equation. 2006 *Braz. J. Phys.* **2006**, *36*, 1285–1289, doi: 10.1590/S0103-97332006000700029.
24. Seifert, U. Entropy production along a stochastic trajectory and an integral fluctuation theorem. *Phys. Rev. Lett*. **2005**, *95*, 040602, doi: 10.1103/PhysRevLett.95.040602.
25. Kawazura, Y.; Yoshida, Z. Entropy production rate in a flux-driven self-organizing system. *Phys. Rev. E* **2010**, 82, 066403, doi: 10.1103/PHYSREVE.82.066403.
26. Martyushev, L. M. The maximum entropy production principle: two basic questions. *Phil. Trans. R. Soc. B* **2010**, 365, 1333, doi: 10.1098/rstb.2009.0295.
27. Dewar, R. C. Information theory explanation of the fluctuation theorem, maximum entropy production and self-organized criticality in non-equilibrium stationary states. *J. Phys. A: Math. Gen.* **2003**, *36*, 631–641, doi: 10.1088/0305-4470/36/3/303.
28. Dewar, R. C. Maximum entropy production and the fluctuation theorem. *J. Phys. A: Math. Gen.* **2005**, *38*, L371–L381, doi: 10.1088/0305-4470/38/21/L01.
29. Bruers, S. A discussion on maximum entropy production and information theory. *J. Phys. A: Math. Theor.* **2007**, *40*, 7441–7450, doi: 10.1088/1751-8113/40/27/003.
30. Dewar, R. C. Maximum entropy production as an inference algorithm that translates physical assumptions into Mmacroscopic predictions: don't shoot the messenger. *Entropy* **2009**, *11*, 931–944, doi:10.3390/e11040931.
31. Ross, J., Corlan, A. D. & Müller, S. C. Proposed principles of maximum local entropy production. *J. Phys. Chem. B* **2012**, *116*, 7858–7865, doi: 10.1021/jp302088y.
32. Presse, S.; Ghosh, K.; Lee, J.; Dill, K. A. Principles of maximum entropy and maximum caliber in statistical physics. *Rev. Mod. Phys.* **2013**, 85, 1115, doi: 10.1103/RevModPhys.85.1115.
33. Doi, M. Onsager's variational principle in soft matter. *J. Phys.: Cond. Matt*. **2011**, *23*, 284118, doi: 10.1088/0953-8984/23/28/284118.
34. Zivieri, R.; Pacini, N.; Finocchio, G.; Carpentieri, M. Rate of entropy model for irreversible processes in living systems. *Sci. Rep.* **2017**, *7*, 9134, doi: 10.1038/s41598-017-09530-5.
35. Zivieri, R.; Pacini, N. Is an Entropy Based Approach Suitable for an Understanding of the Metabolic Pathways of Fermentation and Respiration? *Entropy* **2017**, 19, 662, doi: 10.3390/e19120662.